The x-ray magnetic circular dichroism spin sum rule for $3d^4$ systems: Mn^{3+} ions in colossal magnetoresistance manganites

The x-ray magnetic circular dichroism spin sum rule for 3d^4 systems: Mn^{3+} ions in colossal magnetoresistance manganites

K Kuepper[1,9]**, M Raekers**[2]**, C Taubitz**[2]**, M Uhlarz**[3]**, C Piamonteze**[4]**,
F M F de Groot**[5]**, E Arenholz**[6]**, V R Galakhov**[7]**, Ya M Mukovskii**[8] **and
M Neumann**[2]

[1] Helmholtz-Zentrum Dresden-Rossendorf, Institute of Ion Beam Physics and Materials Research,
PO Box 51 01 19, D-01314 Dresden, Germany
[2] Department of Physics, University of Osnabrück, D-49069 Osnabrück, Germany
[3] Helmholtz-Zentrum Dresden-Rossendorf, High Magnetic Field Laboratory, PO Box 51 01 19, D-01314
Dresden, Germany
[4] Swiss Light Source, Paul Scherrer Institut, CH-5232 Villigen PSI, Switzerland
[5] Department of Inorganic Chemistry and Catalysis, Utrecht University, Sorbonnelaan 16, 3584 CA
Utrecht, The Netherlands
[6] Advanced Light Source, Lawrence Berkeley National Laboratory, Berkeley, CA 94720, USA
[7] Institute of Metal Physics, Russian Academy of Sciences—Ural Division, 620990 Yekaterinburg,
Russia
[8] National Science and Technology University 'MISiS', 119049 Moscow, Russia

E-mail: karsten.kuepper@uos.de

Abstract
The colossal magnetoresistance manganites La$_{0.87\pm0.02}$Sr$_{0.12\pm0.02}$MnO$_{3+\delta}$,
La$_{0.78\pm0.02}$Sr$_{0.17\pm0.02}$MnO$_{3+\delta}$, and La$_{0.66\pm0.02}$Sr$_{0.36\pm0.02}$MnO$_{3+\delta}$ (δ close to 0) were
investigated by using soft x-ray magnetic circular dichroism (XMCD) and magnetometry.
Very good agreement between the values for the average Mn magnetic moments determined
with these two methods was achieved by correcting the XMCD spin sum rule results by means
of charge transfer multiplet calculations, which also suggest a charge transfer of $\sim$50% for
Mn^{4+} and $\simeq$30% for Mn^{3+}. The magnetic moment was found to be localized at the Mn ions
for $x = 0.17$ and 0.36 at 80 K and for $x = 0.12$ in the temperature range from 80 to 300 K. We
discuss our findings in the light of previously published data, confirming the validity of our
approach.

(Some figures may appear in colour only in the online journal)

1. Introduction

X-ray magnetic circular dichroism (XMCD) is one of the most versatile techniques for the study of the internal magnetic structure of magnetic materials. This stems from its element specificity as well as the unique possibility to separate spin and orbital contribution to the magnetic moment by applying

the sum rules developed by Thole [1] and Carra [2]. In order to extract quantitative accurate results, core level spin–orbit coupling and core–valence exchange interactions have to be taken into account [3, 4]. The fundamental issue behind the correction factor is that assumptions used for the orbital sum rule are not fulfilled for the L edges of 3d systems. The reason is that the orbital sum rule implicitly assumes pure L$_3$ and L$_2$ edges. Due to the large 2p3d overlap integrals (a.k.a. multiplet effects), the L$_3$ and L$_2$ edges mix the 2p$_{3/2}$ and 2p$_{1/2}$ character and the orbital sum rule breaks down. To correct for the error

in the sum rule, an alternative procedure is used: (1) the spectrum is fitted with calculations; (2) the orbital moment for the theoretical ground state is determined; (3) the orbital sum rule is applied to the calculated spectra; (4) the error in the orbital sum rule is determined. Therefore, we do not actually use a correction factor, but rather a different procedure to determine the orbital moment. This procedure avoids the error in the orbital sum rule due to multiplet mixing of the *j*-character. These multiplet effects are critical in case of 3d transition metal oxides, in particular for $3d^4$ systems the error of the spin sum rule is very large [4]. Since many $3d^4$ systems exhibit intriguing magnetic properties, e.g. are Cr based ferromagnetic semiconductors [5] or magnetic molecules [6], $SrFeO_3$ based perovskites [7, 8], and in particular the manganese based colossal magnetoresistance perovskites $RE_{1-x}A_xMnO_3$ (where RE and A denote a trivalent rare earth atom and a divalent atom, respectively) [9–11]. Developing a better understanding of the precise internal magnetic structure of such materials and their interfaces [12–17] is of utmost importance.

Here we study a $3d^4$ and a CMR model system, namely $La_{0.87\pm0.02}Sr_{0.12\pm0.02}MnO_{3+\delta}$, $La_{0.78\pm0.02}Sr_{0.17\pm0.02}MnO_{3+\delta}$, and $La_{0.66\pm0.02}Sr_{0.36\pm0.02}MnO_{3+\delta}$ (δ close to 0) by means of XMCD, conventional magnetometry and multiplet simulations including corresponding spin sum rule correction. We demonstrate and validate the spin sum rule correction method developed by Piamonteze *et al* [4] for the particular delicate case of a $3d^4$ system leading to excellent agreement between the results obtained with different methods. Furthermore we compare our results with previously published data [13, 18], demonstrating that previously observed and reported differences using different methods may be resolved by our approach.

2. Experimental and theoretical details

Single crystals of $La_{0.87\pm0.02}Sr_{0.12\pm0.02}MnO_{3+\delta}$, $La_{0.78\pm0.02}Sr_{0.17\pm0.02}MnO_{3+\delta}$, and $La_{0.66\pm0.02}Sr_{0.36\pm0.02}MnO_{3+\delta}$ were grown in air by floating-zone method and details can be found in the work of Shulyatev *et al* [19]. Electron microprobe analysis at different points of the samples reveals a potential deviation from the nominal cation stoichiometry of around 2%, the growth or fritting in air leads to an oxygen content close to 3. A slightly increased oxygen concentration cannot be excluded. The XMCD measurements were performed at beamline 4.0.2 at the Advanced Light Source in Berkeley, California [20, 21], using the eight-pole electromagnet. The experiments were performed within a temperature range of 80–300 K and an external magnetic field of 0.7 T, which was aligned along the *c*-axis of the crystals. The polarity of the field was flipped at each data point measured. Spectra were taken in total electron yield (TEY). The x-ray incident angle was chosen 90° to the sample normal in order to minimize potential self-absorption and electron yield saturation effects. Magnetization measurements were performed with a commercial superconducting quantum interference device (SQUID) magnetometer (Quantum Design MPMS
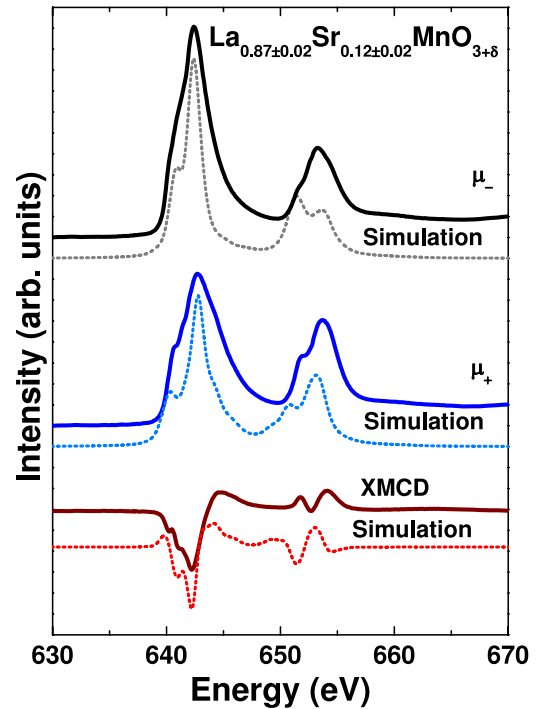

Figure 1. XMCD spectra of $La_{0.87\pm0.02}Sr_{0.12\pm0.02}MnO_{3+\delta}$ with 0.7 T applied magnetic field at 80 K in comparison with charge transfer multiplet calculations.

XL) at the High Magnetic Field Laboratory, Helmholtz-Zentrum Dresden-Rossendorf. The charge transfer multiplet calculations were performed using the TT-multiplet code [22, 23]. The Slater integrals and the spin–orbit couplings were calculated in spherical symmetry and reduced to 80% of the calculated values. Then an octahedral crystal field (10Dq) and an external magnetic field of $\mu_B H = 0.05$ eV along the *z*-direction were applied. Finally charge transfer states were considered. In order to enable a direct comparison between experiment and simulation, the calculated spectra have been normalized to 90% circular polarization by considering the transitions which can only be excited with a linear polarization vector with 10% weight. Furthermore, the calculated spectra have been convoluted with the overall experimental resolution (lifetime broadening plus spectrometer resolution).

3. Results and discussion

Figures 1–3 display the XMCD spectra obtained at 80 K and applied magnetic fields of 0.7 T from $La_{0.87\pm0.02}Sr_{0.12\pm0.02}MnO_{3+\delta}$, $La_{0.78\pm0.02}Sr_{0.17\pm0.02}MnO_{3+\delta}$, and $La_{0.66\pm0.02}Sr_{0.36\pm0.02}MnO_{3+\delta}$. Moreover, charge transfer multiplet calculations assuming a cubic symmetry for the systems are shown as well. For all samples the same parameters were used, but the mixing of Mn^{3+} and Mn^{4+} spectra was derived from the formal valence state determined by the amount of Sr doping. The charge transfer from the ligand oxygen to the Mn site ($3d^n L \rightarrow 3d^{n+1}L^{-1}$) is included in the calculations. The best agreement with the experiment could be achieved with amounts of approximately 50% and 30% for Mn^{4+} and Mn^{3+}, respectively.
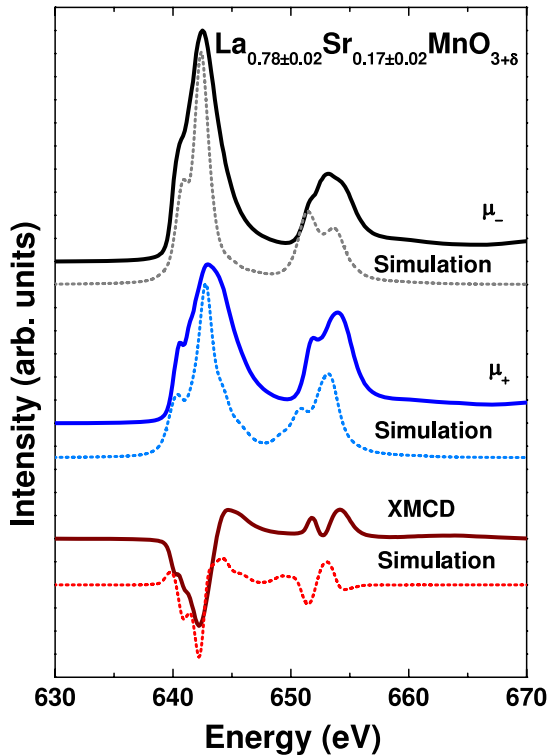
2

Figure 2. XMCD spectra of La$_{0.78\pm0.02}$Sr$_{0.17\pm0.02}$MnO$_{3+\delta}$ with 0.7 T applied magnetic field at 80 K in comparison with charge transfer multiplet calculations.

Figure 3. XMCD spectra of La$_{0.66\pm0.02}$Sr$_{0.36\pm0.02}$MnO$_{3+\delta}$ with 0.7 T applied magnetic field at 80 K in comparison with charge transfer multiplet calculations.

The XMCD spectra show distinct spectral features at the Mn L$_3$ edge near 643 eV and the L$_2$ edge around 654 eV. The main L$_3$ edge feature has two shoulders to lower photon energy (641.5 and 640.5 eV). At higher photon energy a broad shoulder is present (around 645 eV). The main feature of the L$_2$ edge at 653.0 eV has a shoulder at 654.0 eV and a feature at 641.5 eV. A very small feature appears at 650.5 eV. It is very similar for all three samples, but the intensities are slightly different. The feature at 654.0 eV is higher for the sample with a Sr concentration of $x = 0.12$ than for the sample with $x = 0.36$. The shoulder at 640.5 eV is slightly more pronounced for the sample with $x = 0.36$ than for the other two.

The calculations are in overall satisfactory agreement with the experiment, but there are some notable differences. In the positive circularly polarized spectra the main peak at 653.5 eV at the Mn L$_2$ edge is underestimated for all samples, whereas the prepeak located around 651 eV is overestimated in the simulations. Furthermore, the 2p–3d spin–orbit splitting is underestimated approximately by 1 eV in the simulations. The separation between the L$_3$ and the L$_2$ edge is caused by the 2p spin–orbit coupling. In many papers it is assumed that the 2p spin–orbit coupling has its atomic value. However, looking more closely into this issue there are many cases where the experimental difference between the L$_3$ and the L$_2$ edge differs from the theoretical value. The issue is complicated by the fine structure of the L$_3$ and L$_2$ edges, which makes it difficult to determine the L$_3$–L$_2$ splitting precisely. The clearest case is Cu(II), where both the L$_3$ and
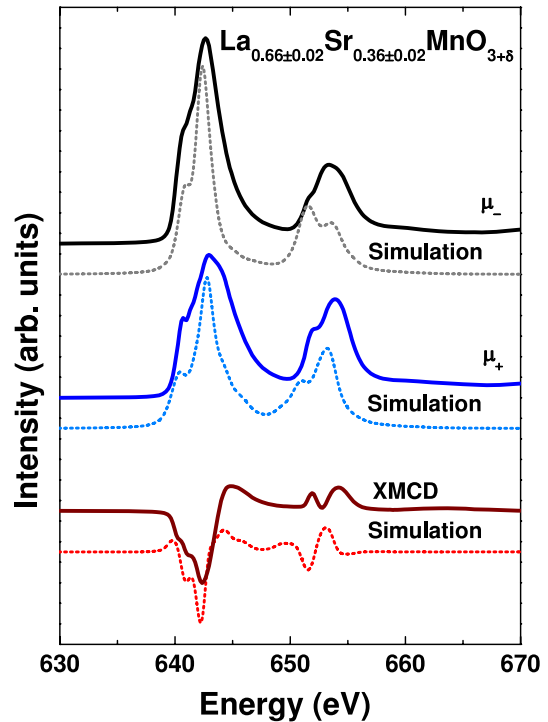
the L$_2$ edge contain a single peak. Experimental values for the 2p spin–orbit splitting range between 19.2 and 20.4 eV, against the theoretical value of 20.3 eV [24]. It is important to notice that the 2p spin–orbit coupling does not play a role in the further discussion of the spin and orbital moment. Instead the 3d spin–orbit coupling is at stake here and is a crucial aspect.

The Mn L$_2$ edge prepeak present in the experimental spectra at 651 eV is hardly visible in the simulations. The prepeak structure of the Mn L$_3$ edge at 641 eV is not completely rendered by the calculation. The different mixing of Mn valence states is overestimated by the calculations in comparison to the experiment. The less pronounced fine structure in the experiment might be considered due to a metallic character of the samples. However, it has been demonstrated before for a very similar system, namely La$_{0.7}$Sr$_{0.3}$MnO$_3$, that dynamical screening leads to a superposition of the electronic structure of initial and final states [25]. Hence, the 2p-hole and the 3d-hole have radial wavefunctions which overlap significantly, and the corresponding Mn L$_{2,3}$ XAS are ruled mainly by (localized) multiplet effects. Nevertheless, the calculation allows us to estimate values for the crystal field (1.4 eV), and the charge transfer amount (Mn^{4+}: 50%, Mn^{3+}: 30%) giving the described agreement with the experiment. This leads to averaged 3.9 holes per Mn ion, which we also used for the sum rule analysis of the experimental spectra. Furthermore, the nonresonant part of the spectra was subtracted by two step functions following the approach of Chen *et al* [26].

For La$_{0.87\pm0.02}$Sr$_{0.12\pm0.02}$MnO$_{3+\delta}$, La$_{0.78\pm0.02}$Sr$_{0.17\pm0.02}$MnO$_{3+\delta}$, and La$_{0.66\pm0.02}$Sr$_{0.36\pm0.02}$MnO$_{3+\delta}$ XMCD spectra

Table 1. Spin and orbital magnetic moment of $La_{0.87\pm0.02}Sr_{0.12\pm0.02}MnO_{3+\delta}$, $La_{0.78\pm0.02}Sr_{0.17\pm0.02}MnO_{3+\delta}$ and $La_{0.66\pm0.02}Sr_{0.36\pm0.02}MnO_{3+\delta}$ at various temperatures and with 0.7 T applied magnetic field extracted from XMCD spectra.

	T (K)	M_{spin} (μ_B)	M_{orb} (μ_B)
$La_{0.87\pm0.02}Sr_{0.12\pm0.02}MnO_{3+\delta}$	80	1.91	0.03 ± 0.01
$La_{0.78\pm0.02}Sr_{0.17\pm0.02}MnO_{3+\delta}$	80	2.21	0.02 ± 0.01
$La_{0.66\pm0.02}Sr_{0.36\pm0.02}MnO_{3+\delta}$	80	1.82	-0.02 ± 0.01
	140	1.54	-0.02 ± 0.01
	150	1.50	0.00 ± 0.01
	160	1.38	0.01 ± 0.01
	180	0.91	0.04 ± 0.01
	200	0.36	0.01 ± 0.01
	220	0.18	0.01 ± 0.01
	250	0.08	0.01 ± 0.01
	300	0.05	0.02 ± 0.01

were measured at temperatures between 80 and 300 K in applied magnetic fields of 0.7 T. The Mn $L_{2,3}$ XMCD spectra are plotted in figure 4. Above 180 K, the dichroism decreases significantly with temperature and nearly vanishes at 220 K while its shape is not changing. In table 1 the spin and orbital magnetic moments extracted using the sum rules are summarized. Since we already used a geometry minimizing self-absorption we did not correct the spectra for electron yield saturation effects. We want to point out that for other transition metal oxides, like Fe_2O_3 or Fe_3O_4 very different values for the electron escape depth have been reported [27, 28], which may influence any potential self-absorption correction in a crucial way.

Theoretically, the orbital sum rule is accurate, and we found only small orbital moments between -0.02 and 0.04 μ_B per Mn atom; similar absolute values have been reported before [12]. Hence the major contribution to the overall magnetization comes from the spin moment. In particular for the $x = 0.12$ sample a sign change of the orbital moment seems to be present at 160 K, which may correspond to a structural phase transition and a subsequent change of the orbital occupation of the 3d e_g level. Such complex behavior of the orbital magnetic moment of orbitally degenerated 3d transition metal ions has been theoretically proposed earlier [29], including the possibility of sign reversal of the orbital moment via interaction with the ligand states in different structural and orbitally ordered or disordered phases [30, 31]. However, on the other hand in many other systems a clear correlation between the spin and the orbital moment has been observed, suggesting at least a reduction of the orbital moment of one order of magnitude (while S is reduced by about two orders). Hence more experiments, in particular similar experiments with opposite helicity will be necessary to ultimately exclude the possibility of any spectral artifacts, e.g. like 'offsets' in the XMCD signal.

In figure 5 the magnetometry data are compared with the magnetic moments at the Mn atoms determined by XMCD and the sum rules. Since the spin sum rule is sensitive to a number of multiplet effects and core–valence interactions for 3d^4 systems as Mn^{3+} ions, we employed the spin sum rule to our multiplet simulations first in order to derive the correction factor accounting for these effects [4]. Following the approach described by Piamonteze *et al* we find spin sum rule correction
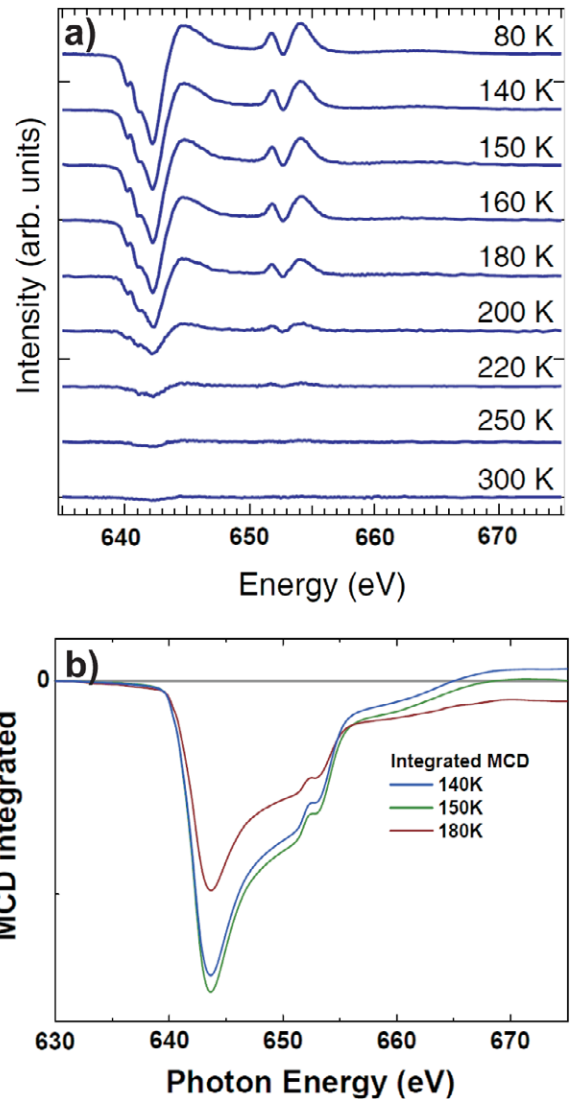
Figure 4. XMCD signals of $La_{0.87\pm0.02}Sr_{0.12\pm0.02}MnO_{3+\delta}$ with 0.7 T applied magnetic field at various temperatures from 80 to 300 K (a), integrals of three selected XMCD spectra (140, 150, and 180 K), demonstrating the sign reversal of the orbital moment (b).

factors of 0.6405 for Mn^{3+} and 0.6075 for Mn^{4+}. Employing these correction factors we find an almost perfect agreement between the overall moments derived from the XMCD sum
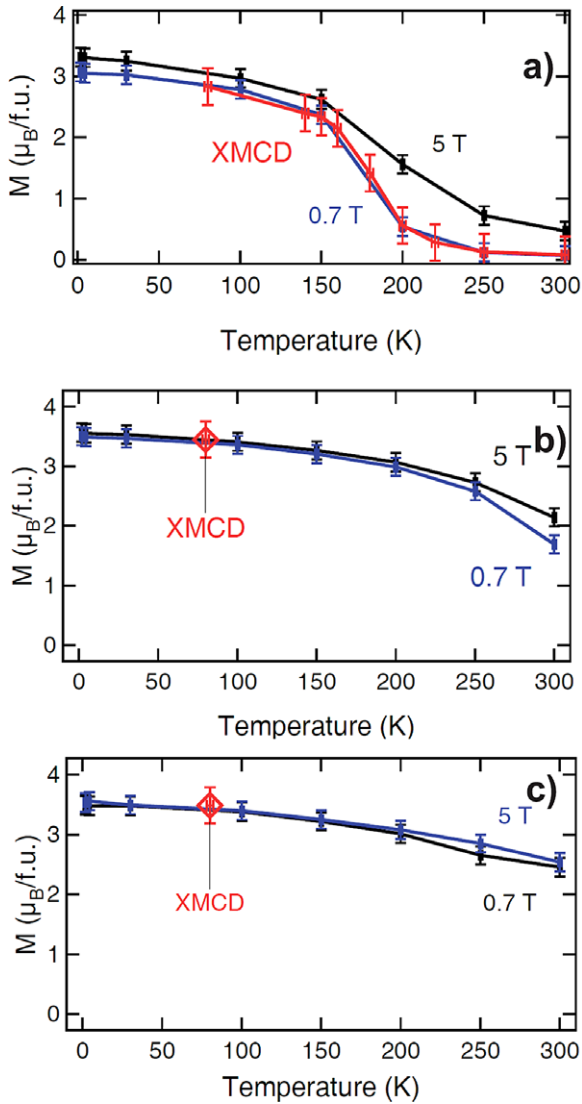
Figure 5. Comparison of magnetic moments of La$_{0.87\pm0.02}$
Sr$_{0.12\pm0.02}$MnO$_{3+\delta}$ (a), La$_{0.78\pm0.02}$Sr$_{0.17\pm0.02}$MnO$_{3+\delta}$ (b), and
La$_{0.66\pm0.02}$Sr$_{0.36\pm0.02}$MnO$_{3+\delta}$ (c) determined by SQUID and
XMCD. The XMCD results were corrected as described in the text.

rules and the magnetometry result (see figure 5). Note that the
3d spin–orbit coupling (ls coupling) was reduced to 25% in
the charge transfer multiplet simulations. A 3d-ls coupling of
100% leads to an error of around 10% of magnetic moments
calculated from the XMCD spectra. Obviously, the Mn^{3+}
(3d^4) configuration is in particular sensitive to the 3d-ls
coupling, since the spin sum rule correction factor is strongly
reduced with 100% 3d-ls coupling (0.5462), whereas the
correction factor for Mn^{4+} ions remains almost unchanged
(0.6066) compared to 25% 3d-ls coupling.

The magnetic moment derived from XMCD data can
also be corrected following a second approach developed
by Teramura *et al* [3]. Using that approach for Mn L edge
XMCD has been very successful in deriving the magnetic
moment in Mn based magnetic molecules [32]. The factor for
Mn^{4+} and Mn^{2+} are 0.68 and 0.587, respectively. We have
approximated the factor for Mn^{3+} as a linear combination of
the factors for 2+ and 4+. We have also taken into account the

charge transfer for Mn^{4+} and Mn^{3+} as used in the multiplet
calculations. This approach leads within 1% deviation to the
same results as the correction factors estimated from our
multiplet simulations.

In figure 5(a) the magnetization of La$_{0.87\pm0.02}$Sr$_{0.12\pm0.02}$
MnO$_{3+\delta}$, La$_{0.78\pm0.02}$Sr$_{0.17\pm0.02}$MnO$_{3+\delta}$, and La$_{0.66\pm0.02}$
Sr$_{0.36\pm0.02}$MnO$_{3+\delta}$ is shown for temperatures from 1.8 to
300 K in fields of 0.7 and 5 T. The magnetic moment at
the Mn atoms determined by XMCD at temperatures from
80 to 300 K at 0.7 T is also presented for comparison.
With the corrections mentioned above an almost perfect
agreement between magnetometry and XMCD could be
achieved. The Curie temperature $T_C = 177$ K determined
by Dabrowski *et al* [33] is also in agreement with our
results. The comparison between magnetometry and XMCD
at 80 K and 0.7 T for La$_{0.87\pm0.02}$Sr$_{0.12\pm0.02}$MnO$_{3+\delta}$,
La$_{0.78\pm0.02}$Sr$_{0.17\pm0.02}$MnO$_{3+\delta}$, and La$_{0.66\pm0.02}$Sr$_{0.36\pm0.02}$
MnO$_{3+\delta}$ is presented in figures 5(b) and (c), respectively. Here
very good agreement between magnetometry and XMCD was
achieved by the corrections mentioned above confirming the
validity of our approach. We want to mention that we did not
consider potential contributions from the other elements to the
total magnetic moment here. Other XMCD studies on very
similar samples revealed only low contributions of the oxygen
atoms [12] and a small spin moment of less than 0.1 μ_B/La
atom [34].

The maximal magnetization of the La$_{0.87\pm0.02}$Sr$_{0.12\pm0.02}$
MnO$_{3+\delta}$, La$_{0.78\pm0.02}$Sr$_{0.17\pm0.02}$MnO$_{3+\delta}$, and La$_{0.66\pm0.02}$
Sr$_{0.36\pm0.02}$MnO$_{3+\delta}$ samples for a temperature of 1.8 K and an
applied field of 5.0 T is 3.31 μ_B/f.u. for $x = 0.12$. This value
seems to be too small in comparison with a simple atomistic
'spin-only guess' for a completely ferromagnetic orientation
of the spins, which gives 3.88 μ_B/f.u. with 12% Mn^{4+} (3 μ_B)
and 88% Mn^{3+} (4 μ_B). For $x = 0.17$ we found for the same
conditions 3.57 μ_B/f.u. which is larger than for $x = 0.12$, but
again smaller than the theoretical value of 3.83 μ_B/f.u. For
$x = 0.36$ the experiment is with 3.53 μ_B/f.u. much closer
to the 'spin-only guess' with 3.64 μ_B/f.u.. Our results for
$x = 0.12$ and 0.17 are in better agreement with neutron powder
diffraction measurements [33] giving $\simeq$3.4 μ_B and $\simeq$3.5 μ_B
for similar Sr concentrations. The too small values could
be explained with cation deficiency and a slightly too high
oxygen content which leads to lower magnetic moments [35],
but also to a change of the Curie temperature. However, these
results demonstrate that the influence of cation deficiency and
oxygen content to the saturation magnetization is not larger
than 15%.

With 3.1 oxygen atoms/f.u. and $\simeq$3.6 μ_B/Mn Bukowski
et al [35] found a decreasing T_C by more than 20 K for a
sample with $x = 0.185$. In the case of our sample with $x =
0.17$ we would achieve a transition temperature $T_C < 260$ K,
which would be observed by our magnetization measurements
(see figure 5, middle panel). Another explanation is given by
Pinsard *et al* [36] finding a spin canting in a sample with
$x = 0.125$ by means of neutron powder diffraction. This effect
is explained with a strong coupling of Jahn–Teller distortion,
ferromagnetic ordering and transport properties. For a higher
Sr concentration the Jahn–Teller distortion becomes smaller

and the difference of the magnetization to the theoretical completely ferromagnetic ordered magnetization disappears. Such a spin canting was also observed by neutron powder diffraction by Xiong *et al* [37] in this Sr concentration range. They found the angle between spin and *c*-axis for $x = 0.11°$ to be $\simeq 77°$. For $x = 0.165\ 40°$ and for $x = 0.185° \simeq 15°$ were determined. Our samples with low Sr concentration are in the range of the coupling between structural and magnetic properties ($0.11 \leq x \leq 0.185$) and the canted spin configuration leads to lower magnetizations than expected for a completely ferromagnetic spin orientation.

　　　Finally we want to compare our results with similar XMCD studies reported in literature. Koide *et al* [13] performed a concentration dependent XMCD study on a series of $La_{1-x}Sr_xMnO_{3+\delta}$ polycrystals. They found discrepancies of 30–40% between the moments derived from the XMCD signal and their SQUID results. Applying our correction factors for Mn^{3+} and Mn^{4+} the error reduces to 10–15%. Whereas the spin sum rule results reveal markedly too low moments, they are too high if one includes the correction factors. The remaining discrepancy may be due to a somewhat inaccurate estimation of the number of holes (they estimated the error to be approx. 10% [13]) and due to inaccuracies stemming from the extraction of the moments from reference [13]. Nevertheless, the discrepancy between the magnetic moments probed by SQUID and XMCD reduces markedly for all samples with one exception ($x = 0.4$). Hence, our spin sum correction factor obviously also improves the results of other measurements performed earlier on similar manganite systems. On the other side Park *et al* [18] probed an $La_{0.3}Sr_{0.7}MnO_3$ thin film by means of XMCD and SQUID. Also they find differences between bulk and surface magnetism, which however is shown to be related to intrinsic properties of the film, e.g. surface stress or finite size effects. However, also for thin film systems, especially if they comprise more than one magnetic element, the application of a spin sum rule correction factor could be of advantage, as already motivated in the introduction.

4. Conclusions

In summary, the average magnetic moments for the compounds $La_{0.87\pm0.02}Sr_{0.12\pm0.02}MnO_{3+\delta}$, $La_{0.78\pm0.02}Sr_{0.17\pm0.02}$ $MnO_{3+\delta}$, and $La_{0.66\pm0.02}Sr_{0.36\pm0.02}MnO_{3+\delta}$ (δ close to 0) were determined using SQUID measurements and XMCD using the spin sum rule correction approach by Piamonteze *et al* [4] and Teramura *et al* [3], taking into account the influence of charge transfer. With this combination of experiments and theory we demonstrate that the spin sum rule correction approach is applicable for the particularly delicate case of $3d^4$ systems, since the spin sum rule error is extremely large for these systems. For the samples with $x = 0.12$ and 0.17, indications for a canted spin configuration are found. The good agreement of the magnetic moment measured by SQUID magnetometry and that determined from XMCD for the single crystalline samples of $La_{0.87\pm0.02}Sr_{0.12\pm0.02}MnO_{3+\delta}$, $La_{0.78\pm0.02}Sr_{0.17\pm0.02}MnO_{3+\delta}$, and $La_{0.66\pm0.02}Sr_{0.36\pm0.02}$ $MnO_{3+\delta}$ indicates that the magnetic moment is, to a large

extent, localized at the Mn ions at 80 K. For $x = 0.12$, the localization is observed in the temperature range from 80 to 300 K.

References

[1] Thole B T, Carra P, Sette F and van der Laan G 1992 *Phys. Rev. Lett.* **68** 1943
[2] Carra P, Thole B T, Altarelli M and Wang X 1993 *Phys. Rev. Lett.* **70** 694
[3] Teramura Y, Tanaka A and Jo T 1996 *J. Phys. Soc. Japan* **65** 1053
[4] Piamonteze C, Miedema P and de Groot F M F 2009 *Phys. Rev. B* **80** 184410
[5] Yamazaki Y *et al* 2011 *J. Phys.: Condens. Matter* **23** 176002
[6] Prinz M *et al* 2010 *Inorg. Chem.* **49** 2093
[7] Okamoto J *et al* 2005 *Phys. Rev. B* **71** 104401
[8] Galakhov V R, Kurmaev E Z, Kuepper K, Neumann M, McLeod J R, Moewes A, Leonidov I A and Kozhevnikov V 2010 *J. Phys. Chem. C* **114** 5154
[9] Millis A J 1998 *Nature* **392** 147
[10] Salamon M B and Jaime M 2001 *Rev. Mod. Phys.* **73** 583
[11] Chuang Y D, Gromko A D, Dessau D S, Kimura T and Tokura Y 2001 *Science* **292** 1509
[12] Pellegrin E, Tjeng L H, de Groot F, Hesper R, Sawatzky G A, Moritomo Y and Tokura Y 1997 *J. Electron Spectrosc. Rel. Phenom.* **86** 115
[13] Koide T *et al* 2001 *Phys. Rev. Lett.* **87** 257201
[14] Chakhalian J *et al* 2006 *Nature Phys.* **2** 244
[15] Arenholz E, van der Laan G, Yang F, Kemik N, Biegalski M D, Christen H M and Takamura Y 2009 *Appl. Phys. Lett.* **94** 072503
[16] Werner R *et al* 2010 *Phys. Rev. B* **82** 224509
[17] Yu P *et al* 2010 *Phys. Rev. Lett.* **105** 027201
[18] Park J-H, Vescovo E, Kim H-J, Kwon C, Ramesh R and Venkatesan T 1998 *Phys. Rev. Lett.* **81** 1953
[19] Shulyatev D, Karabashev S, Arsenov A, Mukovskii Y and Zverkov S 2002 *J. Cryst. Growth* **237** 810
[20] Young A T, Martynov V and Padmore H A 1999 *J. Electron Spectrosc. Relat. Phenom.* **101–103** 885
[21] Young A T, Arenholz E, Feng J, Padmore H, Marks S, Schlueter R, Hoyer E, Kelez C and Steier N 2002 *Surf. Rev. Lett.* **9** 549
[22] de Groot F M F 1994 *J. Electron Spectrosc. Relat. Phenom.* **67** 529
[23] de Groot F M F 2005 *Coord. Chem. Rev.* **249** 31
[24] Sarangi R, Aboelella N, Fujisawa K, Tolman W B, Hedman B, Hodgson K O and Solomon E I 2006 *J. Am. Chem. Soc.* **128** 8286
[25] Wessely O, Roy P, Åberg D, Andersson C, Karis S E, Sanyal B, Svedlindh P, Katsnelson M I, Arvanitis R D and Eriksson O 2003 *Phys. Rev. B* **68** 235109

[26] Chen C T, Idzerda Y U, Lin H-J, Smith N V, Chaban G M, Ho G H, Pellegrin E and Sette F 1995 *Phys. Rev. Lett.* **75** 152

[27] Gota S, Gautier-Soyer M and Sacchi M 2000 *Phys. Rev. B* **62** 4187

[28] Goering E, Gold S, Lafkioti M and Schütz G 2006 *Europhys. Lett.* **73** 97

[29] Hoppe B and Hirst L L 1983 *J. Phys. C: Solid State Phys.* **16** 1919

[30] Galanakis I, Oppeneer P M, Ravindran P, Nordström L, James P, Alouani M, Dreysse H and Eriksson O 2001 *Phys. Rev. B* **63** 172405

[31] Trukhanov S V 2005 *J. Exp. Theor. Phys.* **100** 95

[32] Khanra S *et al* 2008 *Inorg. Chem.* **47** 4605

[33] Dabrowski B *et al* 1999 *Phys. Rev. B* **60** 7006

[34] Kobayashi K, Iwazumi T, Suga S, Imada S, Muro T, Tokura Y and Moritomo Y 1997 *Physica* B **237** 41

[35] Bukowski Z, Dabrowski J, Mais J, Klamut P W, Kolesnik S and Chmaissem O 2000 *J. Appl. Phys.* **87** 5031

[36] Pinsard L, Rodriguez-Carvajal J, Moudden A H and Anane A 1997 *Physica* B **234–236** 856

[37] Xiong X, Dabrowski B, Chmaissem O, Bukowski Z, Kolesnik S, Dybzinski R and Jorgensen J D 1999 *Phys. Rev. B* **60** 10186